

DOI: 10.1002/cbic.200900088

## Functional Analysis of MycE and MycF, Two O-Methyltransferases Involved in the Biosynthesis of Mycinamicin Macrolide Antibiotics

Shengying Li,<sup>[a]</sup> Yojiro Anzai,<sup>[a, b]</sup> Kenji Kinoshita,<sup>[c]</sup> Fumio Kato,<sup>[b]</sup> and David H. Sherman<sup>\*[a]</sup>

Deoxysugars are prevalent structural components of many antibiotics and often contribute substantially to their biological properties.<sup>[1–3]</sup> Methylation of hydroxy group(s) on the deoxy-sugar ring is relatively common (Figure 1), as O-methylation not only protects the reactive hydroxy group from undesired modifications, such as oxidation or dehydration, but also alters the solubility and pharmacokinetic properties of the resulting molecule.<sup>[4]</sup> Biosynthetically, these O-methylation reactions are mainly catalyzed by a variety of S-adenosyl-L-methionine (SAM or AdoMet)-dependent methyltransferases in a site-specific manner. For example, the two SAM-dependent O-methyltransferases TylE and TylF in the tylosin biosynthetic pathway of *Streptomyces fradiae* sequentially methylate individual hydroxy groups (C2'''-OH and C3'''-OH) in the 6-deoxyallose moiety of demethylmacrocin to generate the macrolide antibiotic tylosin.<sup>[5–8]</sup> ElmMI, ElmMII, and ElmMIII are responsible for the consecutive methylation of three hydroxy groups of L-rhamnose in the antitumor polyketide antibiotic elloramycin.<sup>[9]</sup> Moreover, a growing number of O-methyltransferases involved in various deoxysugar methylation reactions such as EryG,<sup>[10]</sup> OleY,<sup>[11]</sup> SpinH, SpinI, and SpinK<sup>[12]</sup> have been reported in diverse antibiotic biosynthetic systems.

Mycinamicins represent a family of macrolide antibiotics with more than 20 members produced by the rare actinomycete *Micromonospora griseorubida*.<sup>[13–15]</sup> The antibacterial activities of some mycinamicin products against *Staphylococcus aureus* are higher than those of the clinical macrolide antibiotics erythromycin and leucomycin. More importantly, mycinamicins have shown strong activity against a number of antibiotic-resistant human pathogens.<sup>[13]</sup> Structurally, the major mycinamicin products of wild-type strain *M. griseorubida* A11725, including mycinamicins I, II, IV, and V, are composed of a 16-membered ring macrolactone core, an N,N-dimethylated deoxysugar desosamine, and a di-O-methylated deoxyhexose mycinose (Figure 1). During the past two decades, the biosynthesis of mycinamicin has been elucidated through strain mutagenesis, bioconversion studies,<sup>[16,17]</sup> and sequence analysis of the complete mycinamicin gene cluster,<sup>[18]</sup> wherein two putative O-

methyltransferase genes *mycE* and *mycF* were tentatively assigned.

Initial bioinformatics analysis of the corresponding genes revealed that MycE and MycF show high amino acid sequence similarities to TylE (demethylmacrocin O-methyltransferase) and TylF (macrocin O-methyltransferase), respectively, in the tylosin biosynthetic pathway.<sup>[18]</sup> Accordingly, the function of MycE was proposed to methylate the C2''-OH group of 6-deoxyallose in mycinamicin VI, leading to mycinamicin III, whereas MycF was presumed to transfer a methyl group to the C3''-OH group of javose (that is, C2''-methylated 6-deoxyallose) in mycinamicin III to generate mycinamicin IV (Scheme 1). The proposed functions of MycE and MycF were supported by in vivo precursor feeding studies.<sup>[16,19]</sup> Herein, we report the expression of *mycE* and *mycF* in *Escherichia coli*, and purification of MycE and MycF to establish their biochemical function for regiospecific deoxysugar O-methylation in mycinamicin macrolide antibiotics.

Comparative analysis revealed that MycE (399 amino acids) is significantly larger than MycF (222 amino acids). Alignment of these two O-methyltransferases exhibits low sequence identity (11.3%), suggesting they might have evolved from distinct ancestors. A protein BLAST search revealed a number of O-methyltransferases with either MycE or MycF as the query protein. Interestingly, all candidates with high sequence similarities are O-methyltransferases involved in deoxysugar biosynthesis. In the phylogenetic tree (Figure 2A) of selected O-methyltransferases with high similarities to MycE and MycF, it is evident that they are located in distinct branches; this indicates their potentially disparate evolutionary origins. In the sequence alignment of MycE with corresponding close relatives (Figure 2B and C), three conserved motifs (motifs I–III)<sup>[9,20]</sup> were identified that are predicted to contribute to SAM binding. In contrast, there are only two conserved SAM binding motifs (motifs I and III) found in MycF.

To confirm the proposed function of MycE and MycF, we cloned *mycE* and *mycF* genes into pET28b for overexpression in *E. coli* BL21 (DE3). The recombinant N-terminal His<sub>6</sub>-tagged proteins were purified to homogeneity by one-step Ni-NTA agarose chromatography (Figure 3). With the purified enzymes in hand, we initially tested the activities of MycE and MycF in sodium phosphate buffer (50 mM, pH 7.4) at 30 °C using SAM as methyl donor and mycinamicin VI and mycinamicin III as substrates (Scheme 1). MycE was unreactive toward both substrates, whereas MycF was able to moderately methylate mycinamicin III (but not VI), forming mycinamicin IV (data not shown). Because the dependence of this class of methyltransferases on a metal cofactor is not uncommon, we next investigated the effect of various divalent metal ions on the activities of MycE and MycF. Both enzymes achieved optimal activity in

[a] S. Li, Dr. Y. Anzai, Prof. D. H. Sherman  
Life Sciences Institute, Department of Medicinal Chemistry,  
Chemistry, and Microbiology and Immunology, University of Michigan  
210 Washtenaw Avenue, Ann Arbor, MI 48109-2216 (USA)  
Fax: (+1) 734-615-3641  
E-mail: davidhs@umich.edu

[b] Dr. Y. Anzai, Prof. F. Kato  
Faculty of Pharmaceutical Sciences, Toho University  
2-2-1 Miyama, Funabashi, Chiba 274-8510 (Japan)

[c] Prof. K. Kinoshita  
School of Pharmaceutical Sciences, Mukogawa Women's University  
11-68 Kyuban-cho, Koshien, Nishinomiya 663-8179 (Japan)

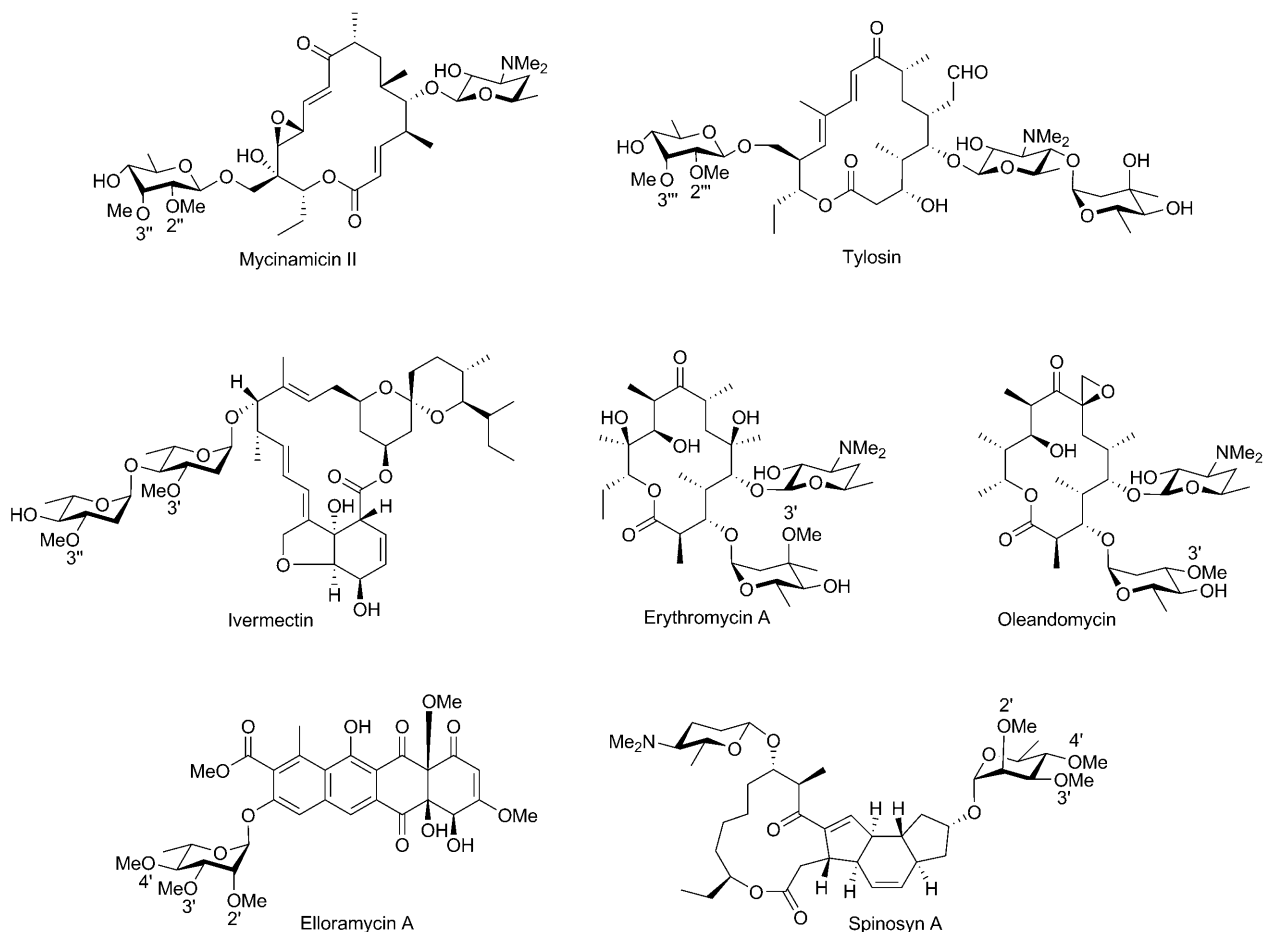
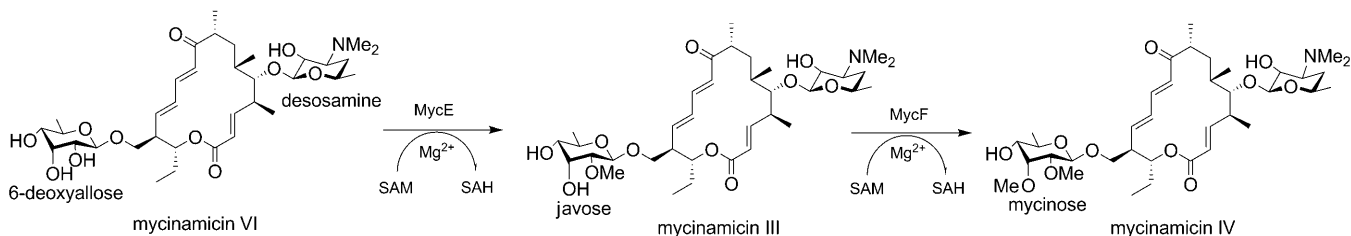


Figure 1. Antibiotics containing various O-methylated deoxysugars. The methyl groups installed by O-methyltransferases are numbered.



Scheme 1. Physiological reactions catalyzed by MycE and MycF.

the presence of 10 mM  $MgCl_2$  (Figure 4A). A number of alternative divalent ions including  $Co^{2+}$ ,  $Fe^{2+}$ ,  $Mn^{2+}$ , and  $Zn^{2+}$  are capable of supporting suboptimal activities. Interestingly, the  $Mg^{2+}$  dependence of MycE appears to be more pronounced than MycF, as MycF remained moderately active in the absence of  $Mg^{2+}$ . The metal dependence of MycF was further assessed by the addition of 2 mM of EDTA; however, this treatment failed to abrogate activity, suggesting that a metal ion might be dispensable in the O-methyltransferase reaction catalyzed by MycF. In contrast, EDTA significantly lowered the activity of MycE even in the presence of 10 mM  $Mg^{2+}$ . The optimal pH and temperature range for MycE and MycF assays were determined through comparison of enzymatic activities under vari-

ous reaction conditions. The optimal reaction conditions of the two O-methyltransferases is pH 9.0 (Figure 4B), significantly higher than the corresponding homologues TyIE (optimal pH 7.5–8.5) and TyIF (pH 7.5–8.0).<sup>[7]</sup> At pH 9.0, the maximal activities of MycE and MycF were observed at 50 and 37 °C (Figure 4C), respectively, higher than those of TyIE (42 °C) and TyIF (31 °C).<sup>[7]</sup>

Under optimal conditions, the *in vitro* activities of MycE and MycF were analyzed to reveal that MycE methylated the C2''-OH of 6-deoxyallose, converting a majority of mycinamicin VI to mycinamicin III (Figure 5B). MycE was incapable of double methylation to generate mycinamicin IV. The second C3''-OH methylation of javose was catalyzed by MycF, with a higher

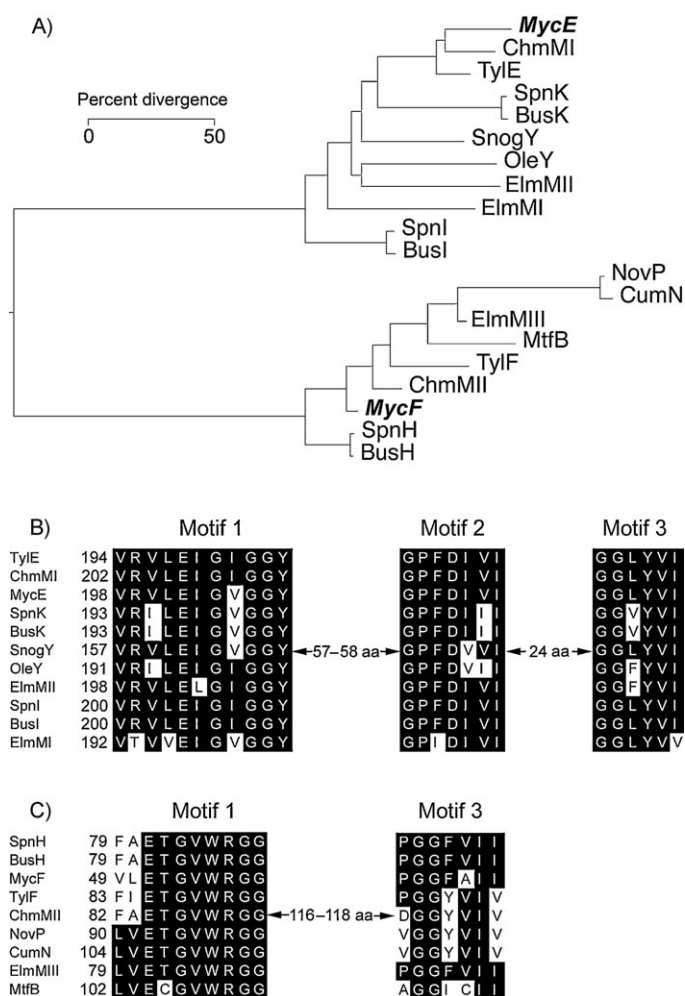


**Figure 2.** Amino acid sequence analysis of MycE and MycF. A) Phylogenetic tree of selected *O*-methyltransferases generated by MegAlign (DNASTAR) with the Clustal W method. MycE and MycF are highlighted in bold and italic. The selected *O*-methyltransferases include MycE and MycF (mycinamicin pathway), TylE and TylF (tylosin pathway), ChmMI and ChmMII (chalcocycin pathway), SpnH, SpnI, and SpnK (spinosad pathway), BusH, BusI, and BusK (butenyl spinosyn pathway), SnogY (nogalamycin pathway), OleY (oleandomycin pathway), ElmMI, ElmMII, and ElmMIII (elloramycin pathway), NovP (novobiocin pathway), CumN (coumermycin pathway), and MtfB (mycobacterial serovar-specific glycopeptidolipid pathway). B) SAM binding motifs of MycE and its homologues. C) SAM binding motifs of MycF and its homologues.

conversion than MycE toward mycinamicin VI (Figure 5F). Co-incubation of MycE and MycF with starting substrate mycinamicin VI resulted in the accumulation of both mycinamicins III and IV (Figure 5D). Notably, mycinamicin IV cannot be further methylated by these two methyltransferases, despite the remaining hydroxy group at the C4'' position in mycinose. Collectively, it is evident that both MycE and MycF possess high substrate specificity.

Finally, we determined the steady-state kinetic parameters (Table 1) for MycE and MycF based on substrate consumption monitored by HPLC. MycE converted mycinamicin VI to mycinamicin III with a  $K_M$  value of  $26.4 \pm 7.0 \mu\text{M}$  and a  $k_{\text{cat}}$  value of  $5.0 \pm 0.5 \text{ min}^{-1}$ . In contrast, MycF methylated mycinamicin III approximately twofold more efficiently (with respect to  $k_{\text{cat}}/K_M$

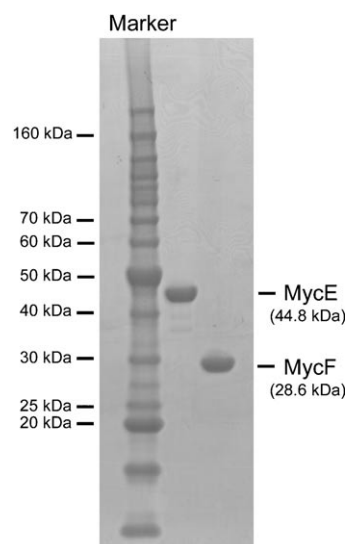


**Figure 3.** SDS-PAGE analysis of purified MycE and MycF.

value) than MycE toward mycinamicin VI. Notably, these kinetic data for MycE and MycF are similar to those of TylE and TylF in the tylosin pathway, as previously reported.<sup>[7]</sup>

The mycinamicin post-PKS (polyketide synthase) tailoring pathway includes two glycosylation steps mediated by two glycosyltransferases (MycB and MycD), four oxidation steps mediated by two cytochrome P450 monooxygenases (MycCI and MycG), and two methylation steps catalyzed by MycE and MycF.<sup>[16]</sup> These post-PKS modifications not only lead to structural diversification, but also confer biologically active properties on the resulting metabolites. We recently confirmed all oxidative tailoring steps in vitro through functional analysis of two P450 enzymes.<sup>[21]</sup> This work revealed the importance of both methylation steps in 6-deoxyallose for substrate recognition by the MycG monooxygenase. In this study, we have advanced the knowledge about this pathway by analyzing MycE and MycF *O*-methyltransferases in vitro. Taking advantage of the reconstituted optimal in vitro assay, the substrate specificity of MycE and MycF and hence the order of sugar modification (mycinamicin VI→III→IV) in this pathway was unambiguously determined. This new information will help facilitate future efforts to manipulate deoxysugar biosynthesis for generation of novel macrolide antibiotics.

## Experimental Section

**MycE and MycF gene cloning:** Using cosmid pMR01<sup>[18]</sup> as template, *mycE* and *mycF* genes were amplified by PCR under standard conditions with primers as follows: forward, 5'-GGA GTT CCA TAT GAC CGC ACA GAC CGA A-3' for *mycE* and 5'-GGA GTT CCA TAT GAG CCC GTC GAC CGG A-3' for *mycF* (bases in italics represent the NdeI cutting site); reverse, 5'-ACA TCA AGC TTT CAT GTC GCG CCT CCG GA-3' for *mycE* and 5'-ACA TCA AGC TTT CAG GCC GAG CGA CGC CA-3' for *mycF* (underlined bases indicate the HindIII restriction site). The gel-purified cDNAs were double digested by NdeI and HindIII (New England Biolabs), followed by the ligation of fragments containing *mycE* and *mycF* genes into NdeI/HindIII-treat-

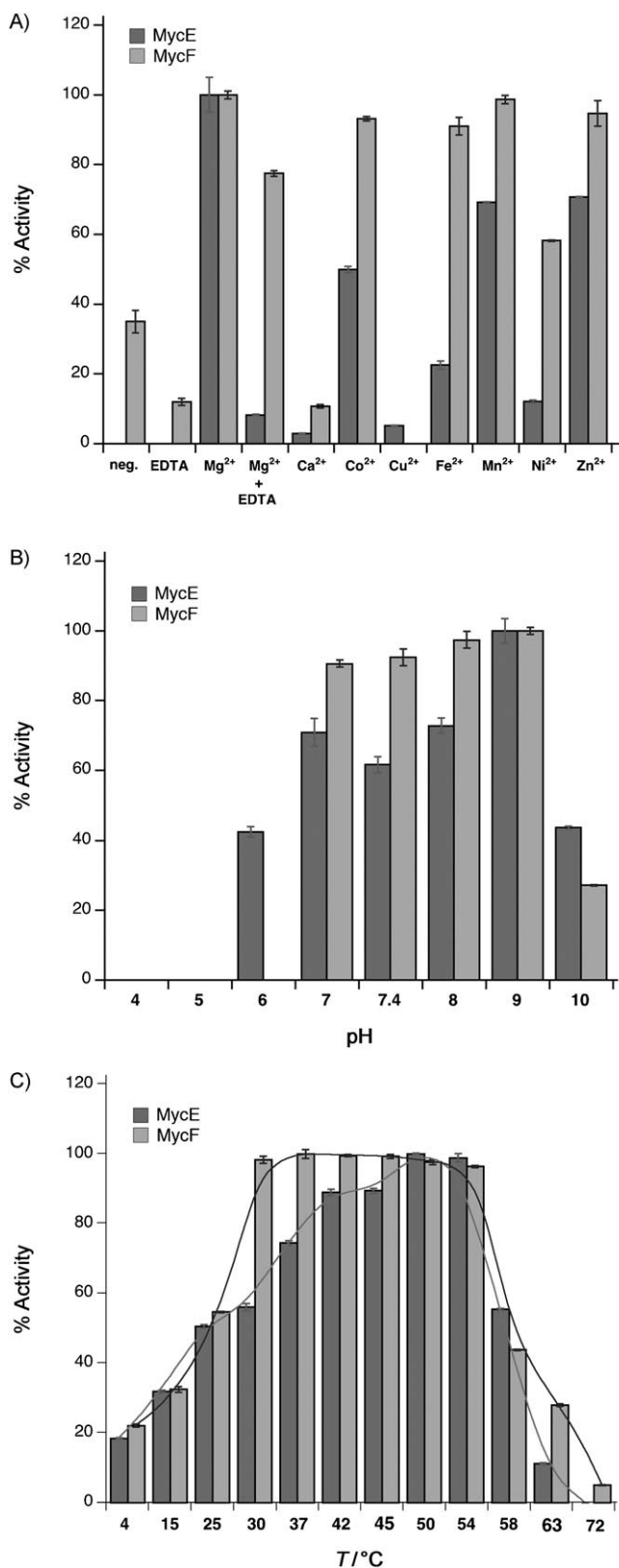


**Figure 4.** Optimization of methylation reactions catalyzed by MycE and MycF. Effects of A) divalent metal ion, B) pH, and C) temperature.

ed pET28b (Novagen) to generate recombinant plasmids pET28b-*mycE* and pET28b-*mycF* for the expression of N-terminal His<sub>6</sub>-

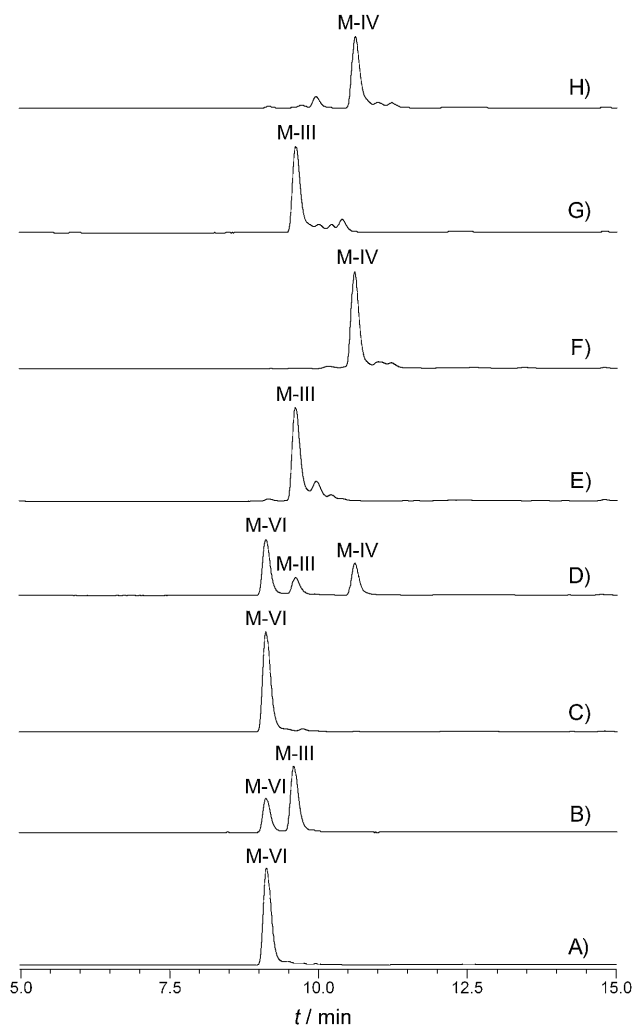


**Figure 5.** LC-MS analysis ( $\lambda = 280$  nm) of in vitro conversions catalyzed by MycE and MycF. A) Mycinamicin VI (M-VI) standard; B) M-VI + MycE; C) M-VI + MycE + MycF; D) M-VI + MycE + MycF; E) mycinamicin III (M-III) standard; F) M-III + MycE; G) M-III + MycE; H) mycinamicin IV (M-IV) standard. Compound identity was confirmed by mass spectrometry and comparison with standard compound regarding retention time and co-injection.

| Table 1. Steady-state kinetic parameters of MycE and MycF. |                         |                                 |  |
|--|-------------------------|---------------------------------|--|
|  | $K_M$ [ $\mu\text{M}$ ] | $k_{cat}$ [ $\text{min}^{-1}$ ] | $k_{cat}/K_M$ [ $\mu\text{M}^{-1} \text{min}^{-1}$ ] |
| MycE   | $26.4 \pm 7.0$          | $5.0 \pm 0.5$                   | 0.19   |
| MycF   | $30.7 \pm 6.9$          | $13.5 \pm 1.1$                  | 0.44   |

tagged MycE and MycF, respectively. The identity of the inserted gene was confirmed by nucleotide sequencing.

**Protein expression and purification:** Recombinant plasmids pET28b-*mycE* and pET28b-*mycF* were used to transform *E. coli* BL21 (DE3) cells with a Z-Competent™ Kit (Zymo Research). The resulting transformants were grown at 37 °C in 1 L of LB broth containing kanamycin ( $50 \mu\text{g mL}^{-1}$ ) for 2–3 h until  $\text{OD}_{600}$  reached 0.6–0.8. Isopropyl- $\beta$ -D-thiogalactopyranoside (IPTG) was then added to a final concentration of 0.1 mM to induce gene expression, and the cells were cultured at 18 °C overnight. The culture was centrifuged

at 5000g for 10 min to collect cells. The freeze–thaw cell pellet was resuspended in 30 mL of lysis buffer (50 mM NaH<sub>2</sub>PO<sub>4</sub>, 300 mM NaCl, 10 mM imidazole, 10% glycerol, pH 8.0) and applied to sonication. Cell debris was removed by centrifugation at 35000g for 30 min, and the supernatant was mixed with 1 mL of Ni-NTA agarose (Qiagen) for 1 h at 4 °C. The slurry was loaded onto an empty column, and the column was washed stepwise with 10 mL of lysis buffer and 40–60 mL of wash buffer (50 mM NaH<sub>2</sub>PO<sub>4</sub>, 300 mM NaCl, 20 mM imidazole, 10% glycerol, pH 8.0). The bound His<sub>6</sub>-tagged proteins were eluted with elution buffer (50 mM NaH<sub>2</sub>PO<sub>4</sub>, 300 mM NaCl, 250 mM imidazole, 10% glycerol, pH 8.0). The MycE (~45 kDa) and MycF (~30 kDa) proteins were further purified and concentrated with 30 kDa and 10 kDa size-exclusion filters (Amicon), respectively. The final desalting step was attained by buffer exchange into storage buffer (50 mM NaH<sub>2</sub>PO<sub>4</sub>, 10% glycerol, pH 7.4) with a PD-10 column (GE Healthcare).

**Enzyme assays:** The optimized enzyme assay was carried out in 100 µL of 50 mM Tris-buffer (pH 9.0) containing 2 µM MycE or MycF, 250 µM substrate (mycinamicin VI for MycE or mycinamicin III for MycF), 10 mM MgCl<sub>2</sub>, and 500 µM SAM at 50 °C (for MycE) or 37 °C (for MycF) for 1 h. The reactions were quenched by extraction with CHCl<sub>3</sub> (2 × 200 µL). The resulting organic extracts were dried and redissolved in 120 µL methanol. LC–MS analysis of the reaction extract was performed with an LC–MS-2010 EV instrument (Shimadzu) by using an XBridge™ reversed-phase HPLC column (C<sub>18</sub>, 3.5 µm, 150 mm; Waters) under the following conditions: 20 → 100% solvent B over 18 min (solvent A = deionized H<sub>2</sub>O + 0.1% formic acid; solvent B = CH<sub>3</sub>CN + 0.1% formic acid), flow rate: 0.2 mL min<sup>-1</sup>, UV wavelength: 280 nm.

**Steady-state kinetics:** The standard reaction buffered with 50 mM Tris-HCl (pH 9.0) contained 0.3 µM MycE or MycF, 500 µM MgCl<sub>2</sub>, 2–100 µM mycinamicin VI for MycE or 3–100 µM mycinamicin III in a total volume of 396 µL. After pre-incubation at optimal temperature for 5 min, the reactions with various substrate concentrations were initiated by adding 4 µL of SAM (50 mM), and three aliquots (100 µL) were taken at three time points (0, 1, 2 min and 0, 2, 4 min for reactions with substrate concentrations < 40 µM and > 60 µM, respectively) within the linear range to thoroughly mix with 100 µL of methanol for reaction termination. The proteins were removed by centrifugation at 16000g for 15 min. The supernatant was subject to HPLC analysis to monitor substrate consumption within the linear range, thereby deducing the initial velocity of the O-methylation reaction. The HPLC conditions were: XBridge™ reversed-phase HPLC column (C<sub>18</sub>, 5 µm, 250 mm; Waters) 20 → 100% solvent B over 20 min (solvent A = deionized H<sub>2</sub>O + 0.1% trifluoroacetic acid; solvent B = CH<sub>3</sub>CN + 0.1% trifluoroacetic acid), flow rate: 1.0 mL min<sup>-1</sup>, UV wavelength: 280 nm. All measurements were performed in duplicate, and velocities determined under different substrate concentrations were fit into the Michaelis–Menten equation to calculate the kinetic parameters.

## Acknowledgements

This work was supported by NIH grant GM078553 and the Hans W. Vahlteich Professorship to D.H.S.

**Keywords:** antibiotics • biosynthesis • deoxysugars • mycinamicin • O-methyltransferases

- [1] C. J. Thibodeaux, C. E. Melancon, H.-w. Liu, *Nature* **2007**, *446*, 1008–1016.
- [2] A. Trefzer, J. A. Salas, A. Bechthold, *Nat. Prod. Rep.* **1999**, *16*, 283–299.
- [3] A. C. Weymouth-Wilson, *Nat. Prod. Rep.* **1997**, *14*, 99–110.
- [4] C. Zubieta, X. He, R. A. Dixon, J. P. Noel, *Nat. Struct. Biol.* **2001**, *8*, 271–279.
- [5] R. Fouces, E. Mellado, B. Diez, J. L. Barredo, *Microbiology* **1999**, *145*, 855–868.
- [6] N. J. Bauer, A. J. Kreuzman, J. E. Dotzlaef, W. K. Yeh, *J. Biol. Chem.* **1988**, *263*, 15 619–15 625.
- [7] A. J. Kreuzman, J. R. Turner, W. K. Yeh, *J. Biol. Chem.* **1988**, *263*, 15 626–15 633.
- [8] N. Bate, E. Cundliffe, *J. Ind. Microbiol. Biotechnol.* **1999**, *23*, 118–122.
- [9] E. P. Patallo, G. Blanco, C. Fischer, A. F. Brana, J. Rohr, C. Mendez, J. A. Salas, *J. Biol. Chem.* **2001**, *276*, 18765–18774.
- [10] T. J. Paulus, J. S. Tuan, V. E. Luebke, G. T. Maine, J. P. DeWitt, L. Katz, *J. Bacteriol.* **1990**, *172*, 2541–2546.
- [11] I. Aguirrezabalaga, C. Olano, N. Allende, L. Rodriguez, A. F. Brana, C. Mendez, J. A. Salas, *Antimicrob. Agents Chemother.* **2000**, *44*, 1266–1275.
- [12] C. Waldron, P. Matsushiba, P. R. Rosteck, M. C. Broughton, J. Turner, K. Madduri, K. P. Crawford, D. J. Merlo, R. H. Baltz, *Chem. Biol.* **2001**, *8*, 487–499.
- [13] I. Sato, N. Muto, M. Hayashi, T. Fujii, M. Otani, *J. Antibiot.* **1980**, *33*, 364–376.
- [14] K. Kinoshita, S. Takenaka, H. Suzuki, T. Morohoshi, M. Hayashi, *J. Antibiot.* **1992**, *45*, 1–9.
- [15] K. Kinoshita, S. Takenaka, M. Hayashi, *J. Antibiot.* **1991**, *44*, 1270–1273.
- [16] H. Suzuki, S. Takenaka, K. Kinoshita, T. Morohoshi, *J. Antibiot.* **1990**, *43*, 1508–1511.
- [17] Y. Anzai, Y. Ishii, Y. Yoda, K. Kinoshita, F. Kato, *FEMS Microbiol. Lett.* **2004**, *238*, 315–320.
- [18] Y. Anzai, N. Saito, M. Tanaka, K. Kinoshita, Y. Koyama, F. Kato, *FEMS Microbiol. Lett.* **2003**, *218*, 135–141.
- [19] M. Inouye, H. Suzuki, Y. Takada, N. Muto, S. Horinouchi, T. Beppu, *Gene* **1994**, *141*, 121–124.
- [20] R. M. Kagan, S. Clarke, *Arch. Biochem. Biophys.* **1994**, *310*, 417–427.
- [21] Y. Anzai, S. Li, M. R. Chaulagain, K. Kinoshita, F. Kato, J. Montgomery, D. H. Sherman, *Chem. Biol.* **2008**, *15*, 950–959.

Received: February 18, 2009

Published online on May 4, 2009